Received 17 July 2023; Accepted 6 September 2023
https://doi.org/10.22226/2410-3535-2023-4-341-346



# Comparison of the results of texture analysis of zirconium alloys based on the data of backscattered electron diffraction and X-ray radiation of different powers

M. G. Isaenkova†, O. A. Krymskaya, K. E. Klyukova, A. V. Bogomolova,
P. S. Dzhumaev, I. V. Kozlov, V. A. Fesenko

†isamarg@mail.ru

National Research Nuclear University "MEPhI", Moscow, 115409, Russia

**Abstract:** The crystallographic texture determines the anisotropy of zirconium alloys and is a sensitive indicator of all processes occurring in materials during plastic deformation, heat treatment, and operation. At present, the development of methods of scanning electron microscopy (SEM), as well as synchrotron radiation diffraction (SRD), makes it possible to significantly simplify the laborious procedure of texture analysis using the traditional X-ray diffraction method based on the results of the "reflection" survey. This work is devoted to the development of methods for quantitative X-ray texture analysis of deformed and annealed zirconium tubes using synchrotron radiation and the comparison of this data with the results obtained by the traditional X-ray texture analysis method. The results of texture analysis performed by different methods are compared. It is shown that when using the SEM and narrow beams of synchrotron radiation, the texture analysis is not very representative. Regularities are established for the improvement of the phase structure in deformed E110 and E635 alloys during annealing in the temperature range 480 – 640°C, as well as some features of the SEM and SRD data. Regularities of recrystallization of the α-Zr-phase in the case of the presence of up to 1.6 wt.% of the β-phase are revealed.

**Keywords:** crystallographic texture, electron microscopy, synchrotron radiation, X-ray radiation

## 1. Introduction

Due to the low thermal neutron capture cross section, high mechanical strength and corrosion resistance in a steam-water medium at temperatures up to 330°C, zirconium alloys are indispensable materials for the core of nuclear water-cooled power reactors [1– 2]. The constant tightening of requirements for the reliability of reactor operation with a simultaneous increase in critical parameters predetermines the need to improve the structure of the used alloys [3 – 5]. The main phase of all zirconium alloys is the α-phase, which is characterized by a hexagonal close packed (HCP) structure [1– 5]. This causes a significant anisotropy of the physical and mechanical properties of single crystals and determines the anisotropy of the operational properties of textured polycrystalline materials: yield strength, radiative growth, thermal and radiative creep, and hydride orientation [6 – 8].

At present, there is a rapid development of new methods for the analysis of crystallographic texture, such as the analysis of the symmetry of the arrangement of Kikuchi lines, which are cones of electron backscattering diffraction (EBSD) from each studied single-crystal region of the sample [9 –11], processing of Debye rings [11–14] obtained by synchrotron studies (SRD) "for transmission" of the thin foils, and the traditional shooting of incomplete direct pole figures (DPF) by X-ray reflection (XRD) from grains of various orientations [15]. All of the above methods make it possible to restore the grain orientation distribution function (ODF). However, these methods have their own advantages and disadvantages. For example, the EBSD method allows one to analyze the structure of only thin layers of annealed alloys with a thickness of about 0.1 μm, while the SRD method makes it possible to characterize both deformed and annealed materials at a depth of 100 –150 μm. In addition, to obtain a statistically significant result, it is necessary to have a reflection from a large number of grains, which is associated with an increase in the duration of the survey. The duration of obtaining Debye rings at one point is 2 – 3 minutes, while EBSD and X-ray methods are performed for several hours.

An increase in the brightness of X-ray radiation and the use of a two-coordinate detector makes it possible to increase the sensitivity of the diffraction analysis of phases present in the material in a small amount (less than 1 wt.%) [16,17]. Two-dimensional diffraction images are analyzed by the modified Rietveld method, which makes it possible to refine microstructure parameters such as fineness, grain size and shape, phase volume fractions, and crystallographic texture [12,18].

The aim of this work was to develop methods for quantitative X-ray texture analysis using synchrotron radiation and to compare its results with the data obtained by the traditional X-ray texture analysis and EBSD-method. The aims of this work were to adapt the methods of quantitative X-ray texture analysis using synchrotron radiation in

relation to zirconium alloys and to compare the results of the synchrotron method with the data obtained by the traditional X-ray one for measuring direct pole figures and by the electron microscopic one of backscattered electron diffraction (EBSD).

## 2. Materials and experimental methods

Development of the algorithm for restoring complete DPFs from Debye rings obtained using synchrotron radiation was performed on model samples of deformed and annealed tubes made of E110 and E635 alloys. The composition of these alloys is presented in the article [10]. The original branch tubes (35 ± 1) mm long were cut off from standard fuel cladding tubes with external and internal diameters of 9.1×7.93 mm from the E110 alloy and standard tubes for guide channels with ones of 12.6×10.9 mm from the E635 alloy.

Since three methods of texture analysis were used: the traditional X-ray method "on reflection", the EBSD method and the method "on transmission" using synchrotron radiation, separate samples shown in Fig. 1 were prepared for each type of study. There are three main directions in a tube: radial (R), tangential (T) and longitudinal or axial (L). In this work, sections perpendicular to the above directions were prepared for the study, we will name them sections R, T and L, respectively.

For the traditional X-ray method, composite R-section samples (Fig. 1b) were prepared from narrow segments shown in Fig. 1a. For the EBSD method, foils were prepared from a plate cut parallel to the tube axis and shown in Fig. 1c. Research on synchrotron radiation was carried out on the foil shown in Fig. 1d. During cutting, each sample was oriented in the goniometric attachment of the machine along the required direction and then cut off using electrical discharge cutting. The obtained section of the sample was ground, polished and etched in order to remove the work-hardened layer formed during electroerosive cutting. For synchrotron and X-ray studies, the removal of work-hardened layers of machined surfaces was carried out by etching in a dilute mixture of nitric and hydrofluoric acids. This sample preparation procedure is described in detail in [10,15,23]. The finished thickness of foils for synchrotron studies was about 100–120 μm. For electron microscopic studies, the surface of the sample was subjected to additional final electropolishing in a solution of $HClO_4 : CH_3OH : C_6H_{14}O_2 =$ $= 1:10:6$ cooled with liquid nitrogen.

Studies of the crystallographic texture were carried out using both the DPF and the ODF. The experimental data for calculating the ODF are either incomplete DPFs (XRD), maps of the distribution of grains by orientations (EBSD method), and Debye rings (SRD). When shooting and constructing DPFs, we used DRON-3 or D8 Discover diffractometers and our own software, described in detail in the work [15]. The construction of complete DPF was carried out by restoring the ODF from four incomplete DPFs (0001), $\{11\bar{2}0\}$, $\{10\bar{1}0\}$, $\{10\bar{1}2\}$ using the LABOTEX software [19,20]. Note that the volume of material involved in the formation of X-ray reflection was $5 \times 2 \times 0.02$ mm$^3$ ($1.6 \times 10^8$ μm$^3$).

For all studied samples, EBSD data were obtained using the EBSD pattern analysis system as part of the Oxford Instruments Nordlys S EBSD pattern detector and the HKL CHANNEL5 software package (Oxford Instruments, UK) based on a Zeiss EVO 50 XVP scanning electron microscope (Carl Zeiss, Germany). The R-section served as the sample coordinate system for EBSD measurements. EBSD scanning was carried out using a step of 0.1–0.2 μm with an average scanning area of $100 \times 80$ μm$^2$, i.e. with a reflecting layer thickness of about 0.1 μm, the investigated volume as a result of scanning the beam over the surface of the R-section was $8 \times 10^2$ μm$^3$. The volume of the studied material in the case of SRD beam diameter of 200 μm was $\pi D^2 h = \pi \cdot 200^2 \cdot 100 = 1.3 \cdot 10^7$ μm$^3$. Thus, the information obtained by the three methods characterizes different volumes and at different depths of the material.

Let us dwell in more detail on the processing of diffraction Debye rings obtained in synchrotron studies. Initially, the diffraction image obtained for the $LaB_6$ powder using synchrotron radiation with a wavelength of 0.74–0.75 Å is processed. The shooting of the $LaB_6$ standard is carried out to refine the parameters of the X-ray radiation of the synchrotron, in particular, the wavelength. Using the ICSD (ICDD), COD, or AMCSD databases, the Rietveld method simulates the diffraction spectrum of textureless $LaB_6$ powder and compares it with the experimental spectrum calculated by summing over Debye rings in the MAUD (Material Analysis Using Diffraction) software [12,13]. The purpose of processing the $LaB_6$ diffraction spectrum is to refine the corresponding instrument parameters that apply to textured samples measured under identical conditions. The error in determining the parameters of the device corresponds to the error in processing the diffraction spectrum of the standard (tuning tool). In this case, the error is about 9%.

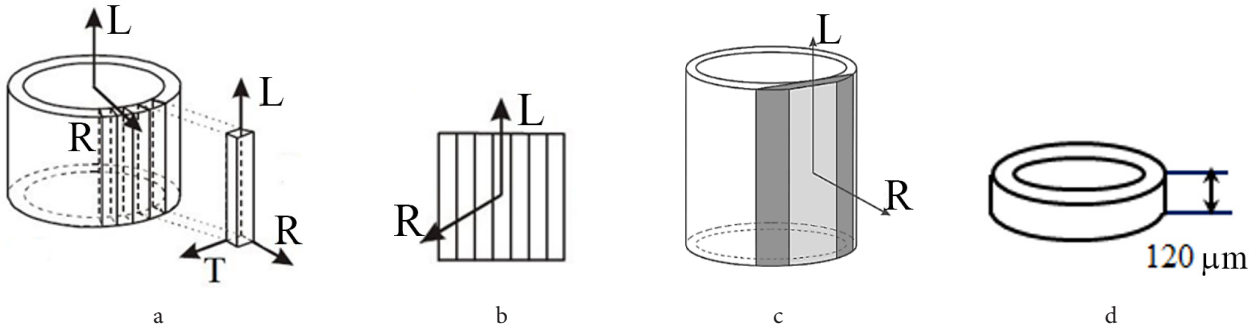


**Fig. 1.** Scheme of preparation of tube samples for studying their texture by different methods: cutting of the original tube on segments (a); composite R-section for shooting "on reflection" (XRD) (b); R-section for measuring with an electron microscope (EBSD) (c); L-section for shooting "on transmission" (SRD) (d).

The diffraction spectra of all the samples of zirconium alloys described above are processed similarly. As an example, in Fig. 2 shows the diffraction Debye rings (Fig. 2 a) and the result of processing the spectrum of a multiphase textured zirconium alloy annealed at a temperature of 520°C for 3 h (Fig. 2 b). According to Fig. 2 b in the annealed E110 alloy, three phases are registered: the main one is a solid solution of alloying elements in the hcp structure of α-Zr, two additional phases are a solid solution Zr in the bcc structure of Nb (β-Nb) and an intermetallic compound with an hcp structure (Laves phase $Zr(Nb, Fe)_2$).

The construction of the DPFs was carried out using the MAUD program [12,13]. The ODFs calculated in the MAUD software were uploaded to the MTEX software [21], which makes it possible to construct complete DPFs and rotate them with respect to external directions.

## 3. Experimental results

Using diffraction spectra obtained with synchrotron radiation, a qualitative and quantitative phase analysis of deformed and annealed tubes from both Russian alloys was made. The reflections found in the diffraction spectra confirmed the previously known phase composition for the E110 alloy: α-Zr, β-Nb, β-Zr (bcc solid solutions with the different Nb and Zr content) and the Laves phase (the intermetallic compound $Zr(Nb, Fe)_2$); for the E635 alloy: α-Zr and the intermetallic compound $Zr(Nb, Fe)_2$. In accordance with the Rietveld method and the PDF2 database, it has been established that the amount of additional phases in Russian zirconium alloys does not exceed 1.6 wt.% in total.

The result of processing the Debye rings of textured samples is the determination of the crystallographic texture and microstructure of each of the phases present in the alloy. The error in determining the phase data includes the error in determining the shooting parameters and the processing errors of a particular sample. The experimentally obtained spectrum and the tabulated values from the cif-file are not perfectly compatible due to experimental errors and counting statistics. In MAUD, after a cycle of refinements, the coincidence error of the calculated and experimental spectra $R$ is reported, which characterizes the sum of the standard deviations of the intensities at each point of the diffraction pattern. Spectrum processing continues until the minimum error $R$ is reached. Evaluation of the errors calculated for all samples shows that the initial refinement is correct if $R$-values change in the range of 5–15% or less [22].

It has been established that with an increase in the annealing temperature, error $R$ increases and its maximum values are reached at 580°C and 600°C, which corresponds to the temperature range of recrystallization of the material with the maximum grain size. Thus, we can conclude that when using the synchrotron method for studying the texture, the data for the deformed sample are restored with a minimum error, and as the grain grows in the annealed materials, the statistics is violated, the error in constructing the ODF increases, and near the annealing temperature of 580°C, the data obtained are the least correspond to the true state of the investigated tubes.

Figures 3 – 4 present the results of studying the texture of the samples of both alloys annealed for 3 hours at a temperature of 480°C and 580°C, respectively. Each figure shows the DPFs (0001), constructed from Debye rings (Fig. 3 a, 4 a), obtained on a DRON-3 diffractometer (Fig. 3 b, 4 b), and also calculated by EBSD map (Fig. 3 c, 4 c).

Fig. 5 shows the distributions of the basal axes in E110 (Fig. 5 a) and E635 (Fig. 5 b) alloys annealed at different temperatures, where ψ is the tilt angle for DPF or Euler angle

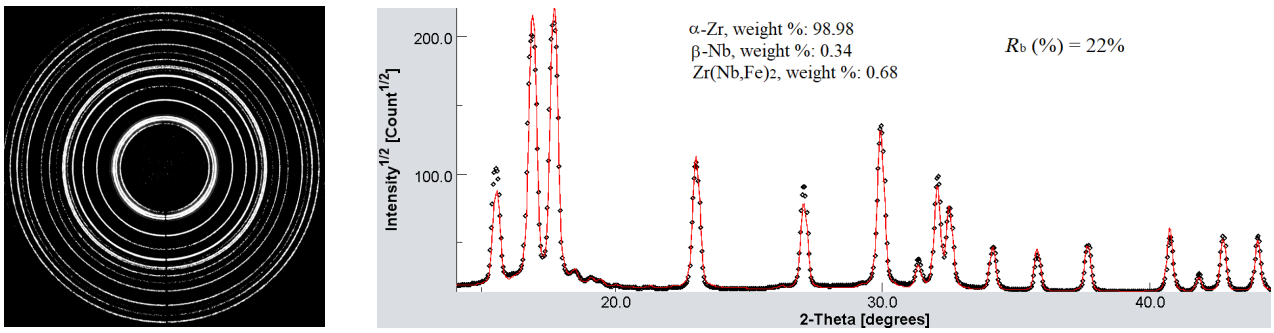


**Fig. 2.** Debye rings (a) and diffraction spectrum (b) of the E110 alloy annealed at 520°C for 3 h.

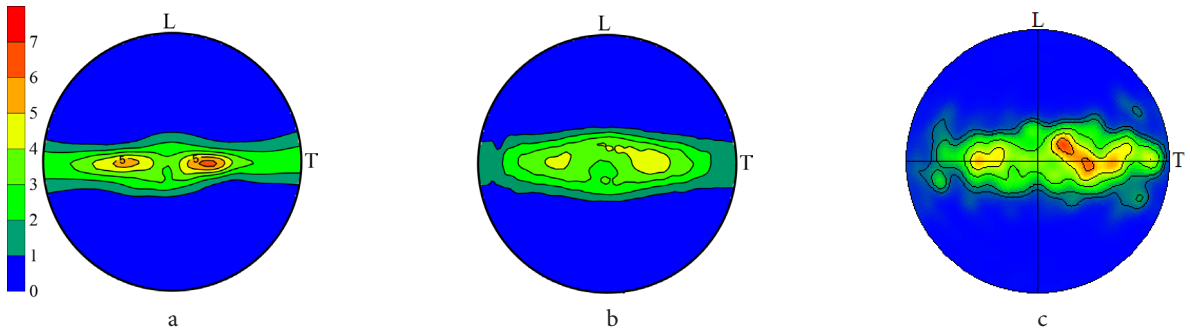


**Fig. 3.** (Color online) DPFs (0001) obtained by the SRD (a), XRD (b) and EBSD methods (c) for the E110 alloy annealed at a temperature of 480°C for 3 hours.

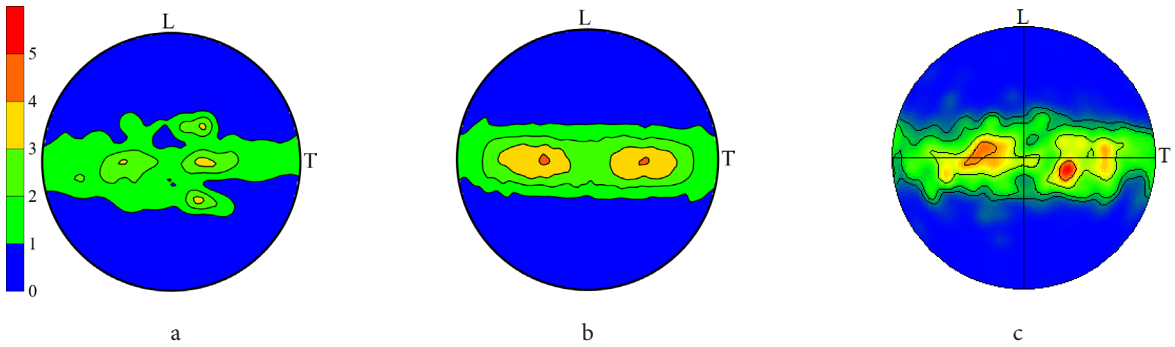


**Fig. 4.** (Color online) DPFs (0001) obtained by the SRD (a), XRD (b) and EBSD methods (c) for the E635 alloy annealed at a temperature of 580°C for 3 hours.

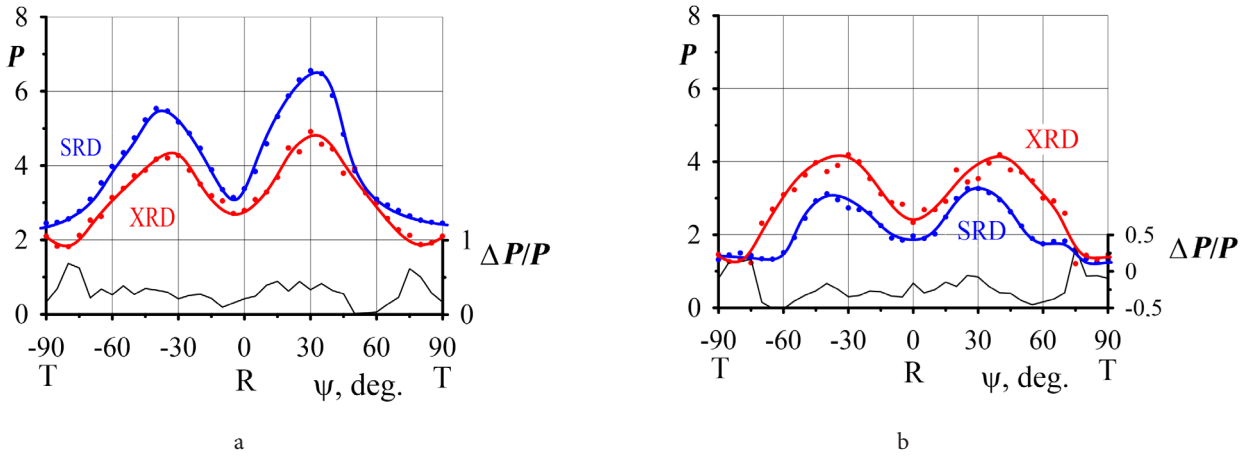


**Fig. 5.** (Color online) Distributions of basal axes in the R-T section constructed from SRD (blue lines) and XRD (red lines) measurements of tubes made of the E110 (a) and E635 (b) alloys annealed for 3 hours at temperatures of 480 and 580°C, respectively. Black thin lines correspond to the deviation of the pole densities calculated from the data of different DPF measurement methods.

Φ for ODF. The distributions are plotted using a synchrotron SRD (a blue line) and an X-ray (XRD) (red one) diffraction. In Fig. 5, a thin black line shows the change in the relative error calculated from the pole densities obtained using the SRD and XRD methods: $\Delta P/P=(P_{SRD}-P_{XRD})/P_{XRD}$. A large decrease in the pole density measured by SRD for the annealed E635 alloy (Fig. 5 a, b) is associated with the appearance of additional texture maxima on the DPF (0001) (see Fig. 4 a).

## 4. Discussion

When processing the results of synchrotron studies, it was found that with an increase in the annealing temperature, the error in processing the diffraction spectra calculated from Debye rings, *R* increases, and its maximum values (reaching 25%) fall at 580 – 600°C, which corresponds to the recrystallization temperature of the material with the maximum grain size. That is, when using the SRD method to study the texture, the data for the deformed sample are restored with a minimum error, and in annealed materials with grain growth at temperatures above 580°C, the statistics are violated and the error in constructing the ODF increases. Therefore, to increase the statistical significance of the results obtained, as well as to reduce the reconstruction error, it is necessary to carry out additional measurements at 2 or 3 points of the sample. However, in this case there are problems with correcting the data for the location of the outer axes, to which the texture is very sensitive.

The main objective of this work was to compare the results of the synchrotron texture analysis with the DPFs obtained by the traditional XRD-method of shooting incomplete DPFs or by EBSD-method. An analysis of the crystallographic texture of the deformed material using EBSD maps cannot be performed. While the other two methods make it possible to construct complete DPFs (0001), {11$\bar{2}$0}, {10$\bar{1}$0}, which agree well with each other (see supplementary materials, Figs. S1 and S2). Therefore, we will compare the results of all three methods for tubes made of different zirconium alloys, which are annealed at a polygonization temperature (480°C) (Fig. 3), i. e. when the deformation texture is preserved in zirconium alloys and the grain does not have time to grow. Further, we will consider the features of DPF (0001) during subsequent recrystallization (580°C) (Fig. 4) [10, 23]. The distribution of basal normals in α-Zr completely determines the anisotropy of the physical and mechanical properties of zirconium products. Therefore, at the first stage of optimizing the algorithm for studying the crystallographic texture of materials using Debye rings obtained on SRD measurements, a comparison was made of the distribution of basal axes on the stereographic projection, which were constructed using the three methods described above. According to the obtained data, the DPF (0001) for the samples cut from the cladding tubes are in good agreement with each other (Fig. 3, S1). According to the presented results, the tube texture is characterized by an axial <10$\bar{1}$0> component (Fig. S1) with a well-pronounced texture maximum deviated from the radial

direction towards the tangential one by an angle of 30 – 40° in deformed and polygonized (annealed at 480°C) tubes (Fig. S2, 5 a). A comparison of the presented data indicates a good reproducibility of the DPFs obtained using radiation of different powers. The latter also indicates the layer-by-layer textural homogeneity of cladding tubes, since the results obtained characterize different layers from 20 to 120 μm. The DPF (0001) obtained from the EBSD map (Fig. 3 c) refers only to the surface layer of the material with a thickness of 0.1 μm and is characterized by a significant asymmetry of the DPF (0001), irregular contours, fragmentation of the main texture maxima and the presence of a large number of additional maxima, which apparently is due to the non-representativeness of the studied volume of material. For this DPF (0001), the number of grains studied was 3175, while in [24] the minimum number of grains required to obtain statistically significant results should be above 25 000. When quantitatively comparing the distributions of the basal normals in the R-T section, one can estimate the error in determining the pole densities $\Delta P/P$ (Fig. 5 a, S2). This error increases with growing temperature and grain size.

With an increase in the annealing temperature, the grain size increases and violations of the statistics are noted not only in the EBSD data, but also in the synchrotron results. As a result, on the DPF (0001) (Fig. 4 a) there is a growth of grains, the basal normals of which deviate significantly from the R-T section to L-direction. According to the previously established trend observed for the recrystallization of the α-matrix of zirconium alloys, the growth of new grains mainly occurs on the slopes of texture maxima, which leads to an increase in their width in the meridional direction [23]. The synchrotron data show grains whose basal normals deviate from the main texture components precisely in the meridional section, in the L-direction. Apparently, the insufficient statistics of synchrotron data makes it possible to register individual grains growing on the slopes of the texture maxima of the deformed material. On the DPF (0001) of the E110 alloy annealed at a temperature of 640°C, i. e. above the monotectoid transformation (see Fig. S3, supplementary material), texture maxima are also observed, which can characterize grains that have undergone phase transformations (PT) $\alpha \rightarrow \beta \rightarrow \alpha$ and are formed in accordance with the Burgers orientation relationship between hcp and bcc structures. Then it can be assumed that new grains deviated significantly from the R-T section of the DPF (0001) were also formed as a result of the inhomogeneity of the PT in the cold-hardened structure of the initial material.

An analysis of the texture of the α-phase using SRD showed that in the bulk of the rolled material there is a deformation texture characteristic of α-Zr (0001)±30-45°R-T<10$\bar{1}$0> (Fig. S1, supplementary material) [10,16,23]. As a result of the recrystallization of α-Zr, the deformation texture is replaced by the recrystallization texture (0001)±30-45°R-T<11$\bar{2}$0> (Fig. S3), which is due to the absorption of the deformed matrix by recrystallized grains misoriented relative to the original grains by turning by 30° around the basal normals, as was shown earlier [10,16,23]. Differences in the texture of recrystallization and deformation were confirmed by the DPF (0001), {11$\bar{2}$0}, {10$\bar{1}$0}, obtained by all considered methods of texture analysis.

Thus, the method of recovering the ODF from the results of processing Debye rings is a very promising procedure for texture analysis. This method can be recommended for assessing the texture of additional phases presented in the alloy in small amounts. To improve the accuracy of the obtained results, it is necessary to increase the number of points under study in the sample, i. e. the volume of the studied material.

## 5. Conclusions

1. Using diffraction spectra obtained with synchrotron radiation, a qualitative and quantitative phase analysis of deformed and annealed tubes made of E110 and E635 alloys was carried out. The phases found in the diffraction patterns confirm the previously known phase composition for the E110 alloy: α-Zr, β-Nb, β-Zr and the Laves phase (intermetallic compound $Zr(Nb,Fe)_2$); for E635 alloy: α-Zr and intermetallic compound $Zr(Nb,Fe)_2$.

2. The algorithm for studying the crystallographic texture of materials using Debye rings obtained with synchrotron X-rays in transmission is optimized for the phase composition of Russian alloys. Orientation grain distribution functions (ODFs) and complete direct pole figures (DPFs) are constructed for the α-phase of deformed E110 and E635 alloys, as well as those annealed at different temperatures in the range of 480 – 640°C.

3. It is shown that the α-Zr rolling texture for the inner layers of the material corresponds to that measured earlier for the surface layers using X-ray analysis, namely, the following texture (0001)±30-45°R-T<10$\bar{1}$0> is observed in the volume of the rolled material. As a result of the recrystallization of α-Zr, the transition of the deformation texture into the recrystallization texture (0001)±30-45°R-T<11$\bar{2}$0> occurs, which is due to the absorption of the deformed matrix by recrystallized grains misoriented with respect to the initial grains by turning by 30° around the basal normals.

4. A comparison of the DPFs obtained using X-rays of different powers and the EBSD method was made. It has been established that X-ray methods are more statistically significant, since they allow obtaining information about grains in larger volumes of the material under study than synchrotron and EBSD methods. Both the synchrotron method and EBSD presented in this study are statistically corrupt methods, so the DPFs obtained using them are similar. Optimization of the synchrotron method by scanning the synchrotron beam over translucent foil and an increase in the area of the investigated surface by the EBSD method will certainly allow obtaining more statistically significant information.

***Supplementary material:*** *The online version of this paper contains supplementary material available free of charge at the journal's website (lettersonmaterials.com).*

***Acknowledgments:*** *The work was carried out with the financial support of the Russian Federation represented by the Ministry of Science and Higher Education of the Russian Federation (Agreement No. 075-15-2021-1352). The authors express their gratitude for the provision of samples for research*

*to the Joint-Stock Company "High-Tech Research Institute of Inorganic Materials named after Academician A. A. Bochvar".*

## References


1. A.S. Zaimovsky, A.V. Nikulina, N.G. Reshetnikov. Zirconium alloys in nuclear power engineering. Moscow, Energoizdat (1994) 256 p. (in Russian)
2. A.V. Nikulina, V.A. Markelov, V.V. Novikov, M.M. Peregud, V.F. Konkov, M.N. Sablin, O.Yu. Mileshkina. VANT series Materials science and new materials. 4 (95), 22 (2018). (in Russian)
3. A.V. Obukhov, G.P. Kobylyanskiy. Tsvetnye metally. 10, 6 (2022). (in Russian) Crossref
4. G.P. Kobylyanskiy, A.O. Mazaev, E.A. Zvir, S.G. Eryomin, E.V. Chertopyatov, A.V. Obukhov. Inorganic Materials: Applied Research. 13 (3), 842 (2022). Crossref
5. S.A. Averin, V.L. Panchenko, V.A. Tsygvintsev, V.I. Pastukhov. Russian Metallurgy (Metally). 2021 (5), 635 (2021). (in Russian) Crossref
6. U.F. Kocks, C.N. Tome, H. R Wenk. Texture and anisotropy. Cambridge University Press (1998) 675 p.
7. K. Geelhood, W.G. Luscher, I.E. Porter. Material Property Correlations: Comparisons between FRAPCON-4.0, FRAPTRAN-2.0, and MATPRO. Pacific Northwest National Laboratory. Report number: PNNL-19417 Rev. 2. Richland. Washington 99352 (2015) 154 p. Crossref
8. M.G. Isaenkova, A.V. Tenishev, O.A. Krymskaya, S.D. Stolbov, V.V. Mikhal'chik, V.A. Fesenko, K.E. Klyukova. Nuclear Materials and Energy. 29, 101071 (2021). Crossref
9. V. Randle, O. Engler. Introduction to Texture Analysis. Macrotexture, Microtexture and Orientation Mapping. Florida, USA, CRC Press LLC (2000) 388 p. Crossref
10. M.G. Isaenkova, K.E. Klyukova, O.A. Krymskaya, V.A. Fesenko, P.S. Dzhumaev. VANT. 1, 15 (2023). (in Russian)
11. S.-P. Tsai, P.J. Konijnenberg, I. Gonzalez, S. Hartke, T.A. Griffiths, M. Herbig, K. Kawano-Miyata, A. Taniyama, N. Sano, S. Zaefferer. Review of Scientific Instruments. 93 (9), 093707 (2022). Crossref
12. L. Lutterotti, R. Vasin, H.-R. Wenk. Powder Diffraction. 29 (1), (2014). Crossref
13. H.-R. Wenk, L. Lutterotti, P. Kaercher, W. Kanitpanyacharoen, L. Miyagi, R. Vasin. Powder Diffraction. 29 (1), 76 (2014). Crossref
14. E.A. Benatti, N.S. De Vincentis, N. Al-Hamdany, N. Schell, H.-G. Brokmeier, M. Avalosa, R.E. Bolmaro. Journal of Synchrotron Radiation. 29, 732 (2022). Crossref
15. Y.A. Perlovich, M.G. Isaenkova, O.A. Krymskaya, V.A. Fesenko. IOP Conf. Ser. Mater. Sci. Eng. 130, 012056 (2016). Crossref
16. M.G. Isaenkova, M.I. Petrov, V.A. Fesenko, N.A. Mikhalyov, I.V. Kozlov. Non-ferrous Metals. 1, 41 (2023). Crossref
17. M.G. Isaenkova, Y.A. Perlovich, S.D. Stolbov, K.E. Klyukova, V.A. Fesenko, E.V. Berlin. Tsvetnye Metally. 2, 68 (2020). (in Russian) Crossref
18. H.M. Rietveld. Z. Kristallogr. 225, 545 (2010). Crossref
19. K. Pawlik. Phys. Stat. Sol. (b). 134, 477 (1986). Crossref
20. LaboTex v. 3.0 by LaboSoft (Krakow, Poland). Available online (accessed on 27 July 2023).
21. MTEX software for analyzing and modeling crystallographic textures by means of EBSD or pole figure data (TU Chemnitz, Germany). Available online (accessed on 27 July 2023).
22. A.I. Saville, A. Creuziger, E.B. Mitchell, S.C. Vogel, J.T. Benzing, J. KlemmToole, K.D. Clarke, A.J. Clarke. Integrating Materials and Manufacturing Innovation. 10, 461 (2021). Crossref
23. K.E. Klyukova, M.G. Isaenkova, O.A. Krymskaya, V.A. Fesenko. Tsvetnye Metally. 10, 19 (2022). (in Russian) Crossref
24. N. Bozzolo, F. Gerspach, G. Sawina, F. Wagner. Journal of Microscopy. 227 (3), 275 (2007). Crossref